SCIENTIFIC REP**O**RTS

OPEN

Two-dimensional Dirac particles in a Pöschl-Teller waveguide

R. R. Hartmann [1] & M. E. Portnoi [2,3]

We obtain exact solutions to the two-dimensional (2D) Dirac equation for the one-dimensional Pöschl-Teller potential which contains an asymmetry term. The eigenfunctions are expressed in terms of Heun confluent functions, while the eigenvalues are determined via the solutions of a simple transcendental equation. For the symmetric case, the eigenfunctions of the supercritical states are expressed as spheroidal wave functions, and approximate analytical expressions are obtained for the corresponding eigenvalues. A universal condition for any square integrable symmetric potential is obtained for the minimum strength of the potential required to hold a bound state of zero energy. Applications for smooth electron waveguides in 2D Dirac-Weyl systems are discussed.

The Pöschl-Teller potential[1] plays an important role in many fields of physics[2] from modeling diatomic molecules and quantum many-body systems[3–5], to applications in astrophysics[6,7], optical waveguides[8] and quantum wells[9,10], through to Bose-Einstein and Fermionic condensates[11,12], and supersymmetric quantum mechanics[13]. For the one-dimensional Schrödinger equation, the hyperbolic symmetric form can be solved in terms of associated Legendre polynomials and the eigenvalues are known explicitly[1,14]. We consider an analogous relativistic problem, that of a two-dimensional Dirac particle, confined by a one-dimensional Pöschl-Teller potential. Several solutions have been obtained for the Dirac equation with central Pöschl-Teller potentials[15–21], and the hyperbolic-secant potential is also known to admit analytic solutions for both the one and two-body one-dimensional Dirac problems[22–24]. Modified Pöschl-Teller potential potentials have also been employed in numerical simulations of potential barriers in bilayer graphene[25].

With the recent explosion of research in Dirac materials[26] there has been a renewed interest in quasi-relativistic phenomena considered in condensed matter systems of different dimensionalities. This is due to the fact that the same equations which govern Dirac fermions in relativity, map directly to the equations of motion describing the quasi-particles in systems such as graphene[27], carbon nanotubes[28], topological insulators[29–31] transition metal dichalcogenides[32] and 3D Weyl semimetals[33]. Massless Dirac particles are notoriously difficult to confine; however, it has been demonstrated that certain types of one-dimensional electrostatic waveguides in graphene, possess zero energy-modes which are truly confined within the waveguide[22,23], and that the number of these zero energy-modes is equal to the number of supercritical states (i.e. bound states whose energy, $E = -M$, where M is the particle's effective mass). Transmission resonances and supercriticality of Dirac particles through one-dimensional potentials have been studied extensively[34–45]. The majority of studies model top-gated carbon-based nanostructures using abrupt potentials[46–56]. However, experimental potential profiles vary smoothly over many lattice constants, with even the smallest of gate generated potentials being far from square[57]. There is also some controversy concerning waveguides which are defined by smoothly decaying, square integrable functions, which decay at large distances as $1/x^n$, where $n > 1$. Numerical experiments imply that such waveguides always contain a zero-energy mode[58], whereas analysis based upon relativistic Levinson theorem, says there is a minimum potential strength required to observe a zero-energy mode[45,59–62]. Our result supports the latter, and we demonstrate this through a simple analysis of supercritical states of zero energy.

In 2D Dirac materials, the low-energy spectrum of the charge carriers can be described by a Dirac Hamiltonian[63] of the form

$$\hat{H} = \hbar v(\sigma_x \hat{k}_x + s_K \sigma_y \hat{k}_y + \sigma_z k_z),$$

(1)

[1]Physics Department, De La Salle University, 2401 Taft Avenue, Manila, 0922, Philippines. [2]School of Physics, University of Exeter, Stocker Road, Exeter, EX4 4QL, United Kingdom. [3]International Institute of Physics, Universidade Federal do Rio Grande do Norte, Natal - RN, Brazil. R. R. Hartmann and M. E. Portnoi contributed equally to this work. Correspondence and requests for materials should be addressed to R.R.H. (email: richard.hartmann@dlsu.edu.ph) or M.E.P. (email: m.e.portnoi@exeter.ac.uk)

where $\hat{k}_x = -i\frac{\partial}{\partial x}$, $\hat{k}_y = -i\frac{\partial}{\partial y}$, $\sigma_{x,y,z}$ are the Pauli spin matrices. v plays the role of the speed of light and k_z is proportional to the particle in-plane effective mass. In graphene, the charge carriers are massless, $k_z = 0$, and the dispersion is linear, $v = v_F \approx 10^6$ m/s is the Fermi velocity and s_K has the value of ± 1 for the K and K' valley respectively[64]. For narrow-gap nanotubes and certain types of graphene nanoribbons[65, 66] the operator $\hat{k}_y$ can by replaced by the number $k_y = E_g/(2\hbar v_F)$, which in the absence of applied field is fixed by geometry, where E_g is the value of the bandgap. For nanotubes, E_g can be controlled by applying a magnetic field along the nanotube axis[24, 67–70]. When k_z is finite, Eq. (1) can be used as a simple model for silicene[71] or Weyl semimetal[26, 72]. It has also been proposed that when graphene is subjected to a periodic potential on the lattice scale, for example, graphene on top of a lattice-matched hexagonal boron nitride[73] the Dirac fermions acquire mass with $E_g = 2\hbar v_F k_z$ being of the order of 53 meV.

In what follows we shall consider a particle described by the Hamiltonian (1) subjected to a one-dimensional potential $U(x)$, which varies on a scale much larger than the lattice constant of the corresponding Dirac material, therefore allowing us to neglect inter-valley scattering for the case of graphene. We shall also set $s_K = 1$, and note that the other valley's wave function can be obtained by exchanging $k_y \rightarrow -k_y$. The Hamiltonian acts on the two-component Dirac wavefunction

$$\Psi = e^{ik_y y}\begin{pmatrix} \Psi_A(x) \\ \Psi_B(x) \end{pmatrix} \tag{2}$$

to yield the coupled first-order differential equations

$$(V - E + M)\Psi_A - i\left(\frac{d}{d\tilde{x}} + \Delta\right)\Psi_B = 0 \tag{3}$$

and

$$(V - E - M)\Psi_B - i\left(\frac{d}{d\tilde{x}} - \Delta\right)\Psi_A = 0. \tag{4}$$

where $\tilde{x} = x/L$ and L is a constant. $V = UL/\hbar v_F$ and the charge carrier energy, ε, have been scaled such that $E = \varepsilon L/\hbar v_F$. The charge carriers propagate along the y-direction with wave vector $k_y = \Delta/L$, which is measured relative to the Dirac point, $\Psi_A(x)$ and $\Psi_B(x)$ are the wavefunctions associated with the A and B sublattices of graphene and finally $M = k_z L$ represents an effective mass in dimensionless units.

In what follows we consider the relativistic quasi-one-dimensional Pöschl-Teller potential problem which can be applied to describe e.g. graphene waveguides. We obtain the exact energy eigenfunctions for this potential and formulate a method for calculating the eigenvalues of the bound states. We then analyze the energy-spectrum of the symmetric Pöschl-Teller potential and obtain expressions for the eigenvalues of the supercritical states. By analyzing the zero-energy supercritical states we obtain a universal threshold condition for the minimum potential strength required for a potential to possess a zero-energy mode, for any square-integrable potential. We also show that the eigenfunctions in the non-relativistic limit restore the one-dimensional Schrödinger equation solutions. Finally, we analyze the eigenvalue spectrum for the modified Pöschl-Teller potential which includes an asymmetry term.

Relativistic one-dimensional Pöschl-Teller problem

In this section we consider the potential

$$V = -\frac{a}{4}[1 - \tanh^2(\tilde{x})] + \frac{b}{2}[1 + \tanh(\tilde{x})], \tag{5}$$

which is a linear combination of the symmetric Pöschl-Teller potential with an additional term which enables the introduction of asymmetry[74]. This potential belongs to the class of quantum models, which are quasi-exactly solvable[23, 75–81], where only some of the eigenfunctions and eigenvalues are found explicitly. The depth of the well is given by $-(a - b)^2/4a$, and the potential width is characterized by the parameter L, which was introduced after Eq. (4). For the case of $b = 0$, the potential transforms into the symmetric Pöschl-Teller potential, while if $a = 0$, the potential is a smooth potential step, which can be used to model a p-n junction[82, 83]. The symmetric and asymmetric forms of the potential are plotted in Fig. 1.

Substituting $\Psi_A = (\Psi_1 + \Psi_2)/2$ and $\Psi_B = (\Psi_1 - \Psi_2)/2$ allows Eqs (3,4) to be reduced to a single second-order differential equation in Ψ_1 (Ψ_2)

$$\left[(V - E)^2 - M^2 - \Delta^2 + is\frac{dV}{d\tilde{x}}\right]\Psi_j + \frac{d^2\Psi_j}{d\tilde{x}^2} = 0, \tag{6}$$

where $s = -(-1)^j$ and $j = 1, 2$ correspond to the spinor components Ψ_1 and Ψ_2 respectively. By making the natural change of variable $Z = [1 + \tanh(\tilde{x})]/2$ and using the wave function of the form $\Psi_j = \exp(pZ)Z^n(1 - Z)^m\psi_j(Z)$ allows Eq. (6) to be reduced to the Heun confluent equation[84] in variable Z:
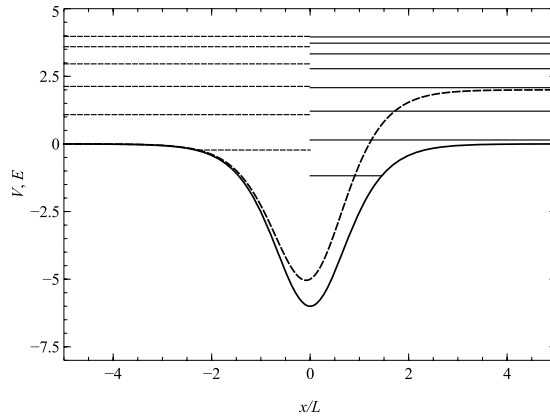
Figure 1. The solid line shows the modified Pöschl-Teller potential, Eq. (5), for the symmetric case of $a = 24$ and $b = 0$. The dashed line shows the asymmetric potential for the case of $a = 24$ and $b = 2$. The 8 solid horizontal lines are the bound state energy levels for the symmetric potential at $\Delta = 4$ and the 6 dashed horizontal lines are the bound state energy levels for the asymmetric potential at $\Delta = 4$.

$$\frac{\partial^2 \psi_j}{\partial Z^2} + \frac{\alpha Z^2 + (2 - \alpha + \beta + \gamma)Z - 1 - \beta}{Z(Z-1)} \frac{\partial \psi_j}{\partial Z}$$
$$+ \frac{[(2 + \beta + \gamma)\alpha + 2\delta_s]Z - (1 + \beta)\alpha + (1 + \gamma)\beta + \gamma + 2\eta_s}{2Z(Z-1)} \psi_j = 0, \quad (7)$$

where $n = \beta/2$, $m = \gamma/2$, $P = \alpha/2$, $\tilde{\Delta}^2 = M^2 + \Delta^2$, $s_{\alpha,\beta\gamma} = \pm 1$ and the parameters α, β, γ, δ_s and η_s are: $\alpha = ias_\alpha$, $\beta = s_\beta \sqrt{\tilde{\Delta}^2 - E^2}$, $\gamma = s_\gamma \sqrt{\tilde{\Delta}^2 - (E-b)^2}$, $\delta_s = a\left(\frac{1}{2}b - is\right)$ and $\eta_s = \beta^2/2 - (a - b)(E - is)/2$. This same method of reducing a system of coupled first-order differential equations to the Heun confluent equation has been exploited to solve various generalisations of the quantum Rabi model[85], and notably the quasi-exact solutions of the Pöschl-Teller family potentials and Rabi systems are closely related[86]. In some instances, the resulting Heun confluent functions can be terminated as a finite polynomial[23, 87], allowing particular eigenvalues to be obtained exactly, providing the parameters obey special relations. When this is not the case, the energy spectrum can be obtained fully via the Wronskian method[23, 85, 88, 89], which is the method we shall utilize.

Equation (7) has regular singularities at $Z = 0$ and 1, and an irregular one at $Z = \infty$ which is outside the domain of $\tilde{x}$. The solutions to Eq. (7) are given by

$$\psi_j = \sum_{s_\alpha, s_\beta, s_\gamma} A_{j, s_\alpha, s_\beta, s_\gamma} H(\alpha, \ \beta, \ \gamma, \ \delta_s, \ \eta_s; \ Z) + B_{j, s_\alpha, s_\beta, s_\gamma} Z^{-\beta} H(\alpha, \ -\beta, \ \gamma, \ \delta_s, \ \eta_s; \ Z), \quad (8)$$

where $A_{j, s_\alpha, s_\beta, s_\gamma}$ and $B_{j, s_\alpha, s_\beta, s_\gamma}$ are constants, and H is the Heun confluent function[90], which has a value of 1 at the origin. For $|Z| < 1$, $H(\alpha, \ \beta, \ \gamma, \ \delta_s, \ \eta_s, \ Z) = (1 - Z)^{-\gamma} H(\alpha, \beta, \ -\gamma, \delta_s, \eta_s, Z)$ and $H(\alpha, \ \beta, \ \gamma, \ \delta_s, \ \eta_s, \ Z) = \exp(-\alpha Z) H(-\alpha, \ \beta, \ \gamma, \ \delta_s, \ \eta_s, \ Z)$, therefore, as expected from the general theory of second order differential equations, the full solution is given by a linear combination of just two linearly independent functions

$$\Psi_j = \left[A_j H(\alpha, \ \beta, \ \gamma, \ \delta_s, \ \eta_s, \ Z) Z^{\frac{1}{2}\beta} + B_j H(\alpha, \ -\beta, \ \gamma, \ \delta_s, \ \eta_s, \ Z) Z^{-\frac{1}{2}\beta} \right] (1 - Z)^{\frac{1}{2}\gamma} \exp\left(\frac{1}{2}\alpha Z\right), \quad (9)$$

where β is not an integer. It should be noted that when $a = 0$ and $\alpha = \delta = 0$, the Heun confluent functions appearing in Eq. (9) reduces to a Gauss hypergeometric functions and for the case of a massless particle Eq. (9) reduce down to the solutions obtained in ref. [82]. If, however, β is an integer then $H(\alpha, -\beta, \gamma, \delta, \eta_s, Z)$ is divergent and B_i has to be set to zero, and the second linearly independent solution can be constructed from a series expansion about the point $1 - Z$. The solutions to the Heun confluent equation thus far have been given as power series expansions about the point $Z = 0$. However, these power series rapidly diverge as Z approaches the second singularity; therefore, at $Z = 1$ we must construct solutions as power series expansions in variable $1 - Z$:

$$\Psi_j = [C_j H(-\alpha, \ \gamma, \ \beta, \ -\delta_s, \ \eta_s + \delta; \ 1 - Z)(1 - Z)^{\frac{1}{2}\gamma} + D_j H(-\alpha, \ -\gamma, \ \beta,$$
$$-\delta_s, \ \eta_s + \delta; \ 1 - Z)(1 - Z)^{-\frac{1}{2}\gamma}] \times Z^{\frac{1}{2}\beta} \exp\left(\frac{1}{2}\alpha Z\right). \quad (10)$$

The constants C_i and D_i are found by matching the two power series expansions and their derivatives at Z_0 where $0 < Z_0 < 1$.

For bound states, we require that $\tilde{\Delta}^2 > E^2$ and $\tilde{\Delta}^2 > (E - b)^2$. These conditions ensure that the bound states are inside the effective bandgap (which accounts for the motion along the y-axis). As $x \to -\infty$, $Z \to 0$ and as $x \to \infty$, $Z \to 1$, therefore we may write the asymptotic expressions of Ψ_j as

$$\lim_{Z \to 0}\left(\Psi_j\right) = A_j Z^{\frac{1}{2}\beta} + B_j Z^{-\frac{1}{2}\beta} \tag{11}$$

and

$$\lim_{Z \to 1}\left(\Psi_j\right) = \left[C_j(1 - Z)^{\frac{1}{2}\gamma} + D_j(1 - Z)^{-\frac{1}{2}\gamma}\right]\exp\left(\frac{1}{2}\alpha\right). \tag{12}$$

Therefore, for bound states, B_i (A_i) is zero for $s_\beta = 1$ ($s_\beta = -1$) and D_i (C_i) is zero for $s_\gamma = 1$ ($s_\gamma = -1$). Clearly the choice of s_β and s_γ is arbitrary, therefore, from hereon in we set both to 1 unless otherwise stated. In this instance, the energy eigenvalues are found from the condition:

$$\frac{\partial H(\alpha, \beta, \gamma, \delta_s, \eta_s, Z)}{\partial Z}\bigg|_{Z_0} H(-\alpha, \gamma, \beta, -\delta_s, \eta_s + \delta; \ 1 - Z_0)$$
$$= \frac{\partial H(-\alpha, \gamma, \beta, -\delta_s, \eta_s + \delta; \ 1 - Z)}{\partial Z}\bigg|_{Z_0} H(\alpha, \beta, \gamma, \delta_s, \eta_s, Z_0), \tag{13}$$

where $0 < Z_0 < 1$.

Symmetric Pöschl-Teller potential solutions. In general, relating Ψ_1 to Ψ_2 is non-trivial, since neither a known expression exists which connects Heun confluent functions about two different singular points for arbitrary parameters, nor is there a general expression relating the derivative of the confluent Heun function to other confluent Heun functions, though particular instances have been obtained[91, 92]. However, for the symmetric Pöschl-Teller potential (i.e. $b = 0$) one can obtain the relation:

$$2Z(1 - Z)\frac{dH(\alpha, \beta, \gamma, \delta_1, \eta_1, Z)}{dZ} = (\beta - iE)H(\alpha, \beta, \gamma, \delta_{-1}, \eta_{-1}, Z)$$
$$+ [(\beta + \gamma)Z - (\beta - iE) - (\alpha + \delta_1)Z(1 - Z)]$$
$$H(\alpha, \beta, \gamma, \delta_1, \eta_1, Z). \tag{14}$$

Therefore, $A_2 = \Omega_{s_\beta} A_1$ and $B_2 = \Omega_{-s_\beta} B_1$, where $\Omega_{s_\beta} = (E + i\beta)/(M + i\Delta)$.

In pristine graphene, only the symmetric form of Eq. (5) will contain non-leaky modes at zero energy. Non-zero-energy modes will have a finite lifetime since they can always couple to continuum states outside of the waveguide, whereas zero-energy modes are fully confined since the density of states vanishes at zero energy outside of the well. Asymmetric forms of Eq. (5) never contain truly bound modes since the density of states cannot vanish on both sides of the potential simultaneously. Notably, this is somewhat counterintuitive as for the Schrödinger problem a symmetric potential always contains a bound state, which can be removed by asymmetry. The emergence of bound states for a relativistic problem with an infinitely wide barrier is a manifestation of the Klein tunneling phenomenon[22, 23].

We shall now consider the symmetric form of Eq. (5) for massless particles. Accordingly, we set $b = 0$ and $M = 0$, and in this instance the symmetrized real functions[22, 23], are given by $\Psi_\mathrm{I} = \Psi_A + i\Psi_B$ and $\Psi_\mathrm{II} = \Psi_A - i\Psi_B$, where

$$\Psi_A = A_1 \Re\left[\Phi\exp\left(\frac{1}{2}\alpha Z - i\frac{\theta}{2}\right)\right] Z^{\frac{1}{2}\beta}(1 - Z)^{\frac{1}{2}\gamma}\exp\left(i\frac{\theta}{2}\right) \tag{15}$$

and

$$\Psi_B = iA_1 \Im\left[\Phi\exp\left(\frac{1}{2}\alpha Z - i\frac{\theta}{2}\right)\right] Z^{\frac{1}{2}\beta}(1 - Z)^{\frac{1}{2}\gamma}\exp\left(i\frac{\theta}{2}\right), \tag{16}$$

where $\Phi = H(\alpha, \beta, \gamma, \delta_1, \eta_1, Z)$ and $\tan\theta = -E/\beta$. By employing the identity Eq. (14), the derivatives appearing in Eq. (13) can be expressed in terms of Heun confluent functions. It immediately follows that at the origin $\Psi_\mathrm{I}^*\Psi_\mathrm{II} + \Psi_\mathrm{I}\Psi_\mathrm{II}^* = 0$, which in terms of the functions Ψ_A and Ψ_B yields:

$$\left|\Psi_A\left(Z = \frac{1}{2}\right)\right|^2 = \left|\Psi_B\left(Z = \frac{1}{2}\right)\right|^2, \tag{17}$$

where $Z = 1/2$ corresponds to $x = 0$. Substituting Eq. (15) and Eq. (16) into Eq. (17) results in the condition

$$\Re\left[\Phi\left(Z = \frac{1}{2}\right)\exp\left(\frac{\alpha}{4} - i\frac{\theta}{2}\right)\right] \mp \Im\left[\Phi\left(Z = \frac{1}{2}\right)\exp\left(\frac{\alpha}{4} - i\frac{\theta}{2}\right)\right] = 0. \tag{18}$$

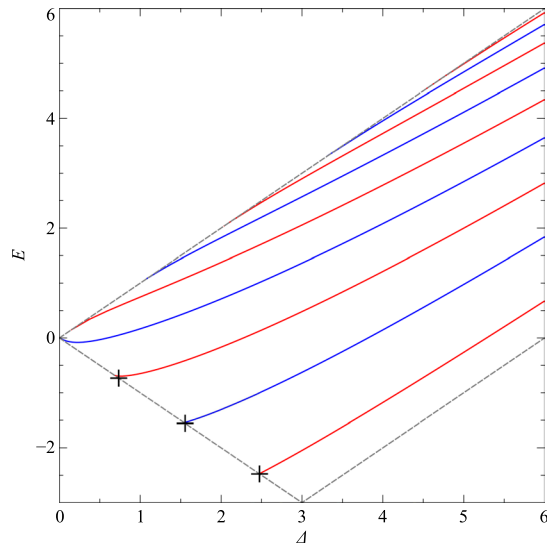**Figure 2.** The energy spectrum of confined states in the symmetric Pöschl-Teller potential, of strength $a = 24$, as a function of Δ. The alternating red and blue lines represent the odd (even) and even (odd) modes of Ψ_I (Ψ_{II}) respectively. The black crosses denote the supercritical states. The boundary at which the bound states merge with the continuum is denoted by the grey (short-dashed) lines.

From Eq. (15) and Eq. (16), $A_1\Psi_A^* = A_1^*\Psi_A \exp(-i\theta)$ and $A_1\Psi_B^* = -A_1^*\Psi_B \exp(-i\theta)$. Therefore, the condition from which the eigenvalues of the spectrum are determined, Eq. (17), can be written as $(\Psi_A + i\Psi_B)|_{Z=\frac{1}{2}}$ $(\Psi_A - i\Psi_B)|_{Z=\frac{1}{2}} = 0$. This condition can be understood in terms of parity. In principle, one can construct from these functions odd and even solutions. However, since the even modes of Ψ_I occur at the same energies as the odd modes of Ψ_{II} and vice versa, one can obtain the eigenvalues when the symmetrized functions Ψ_I or Ψ_{II} are zero at the origin. The functions Ψ_I and Ψ_{II} are related to the earlier introduced functions Ψ_1 and Ψ_2 by

$$\Psi_I = \frac{1}{2}[(1+i)\Psi_1 + (1-i)\Psi_2] \tag{19}$$

and

$$\Psi_{II} = \frac{1}{2}[(1-i)\Psi_1 + (1+i)\Psi_2]. \tag{20}$$

Using Eqs (19, 20) together with Eqs (9),(10) allows Ψ_I and Ψ_{II} to be expressed explicitly in terms of Heun functions.

Eq. (18) is formally the same as Eq. (13) but computationally faster. In Fig. 2 we plot the numerically obtained solutions of Eq. (18) for the potential defined by $a = 24$ and $b = 0$. The dashed lines represent the boundary at which the bound states merge with the continuum which occurs at the energies $E = \pm\Delta$ and $E + a/4 = \Delta$. For the potential of strength $a = 24$ we find that there are four zero-energy bound modes, occurring at $\Delta = 0.597, 2.276, 3.817$ and 5.282. Their normalized wavefunctions are shown in Fig. 3.

As mentioned previously, the number of zero-energy modes is equal to the number of supercritical states (neglecting the spin and valley degrees of freedom). For the symmetric Pöschl-Teller potential, the eigenvalues of these supercritical states can be determined approximately, via simple analytic expressions. Moving to the symmetric basis, $(\Psi_I, \Psi_{II})^T$, allows the pair of coupled first order differential equations, Eq. (3) and Eq. (4) to be reduced to a single second order differential equation in Ψ_{II}:

$$[(V-E)^2 - \Delta^2]\Psi_{II} - \frac{1}{(V-E-\Delta)}\frac{dV}{d\tilde{x}}\frac{d\Psi_{II}}{d\tilde{x}} + \frac{d^2\Psi_{II}}{d\tilde{x}^2} = 0. \tag{21}$$

For supercritical states, $E = -\Delta$, Eq. (21) transforms into the differential equation for the angular prolate spheroidal wave functions[93]:

$$\frac{d}{d\eta}\left[(1-\eta^2)\frac{d}{d\eta}S_{1N}(c,\eta)\right] + \left[\lambda_{1N} - c^2\eta^2 - \frac{1}{1-\eta^2}\right]S_{1N}(c,\eta) = 0, \tag{22}$$

where $\eta = \tanh(z)$, $c = \pm V_0$, $\Psi_{II} = \sqrt{1-h^2}\,S_{1N}$, and S_{1N} are the spheroidal wave functions. $\lambda_{1N} = a(a - 8\Delta)/16$, where the permissible values of λ_{1N} must be determined to assure that $S_{1N}(c,\eta)$ are finite at $\eta = \pm 1$. The permissible λ_{1N} can be obtained via the asymptotic expansion
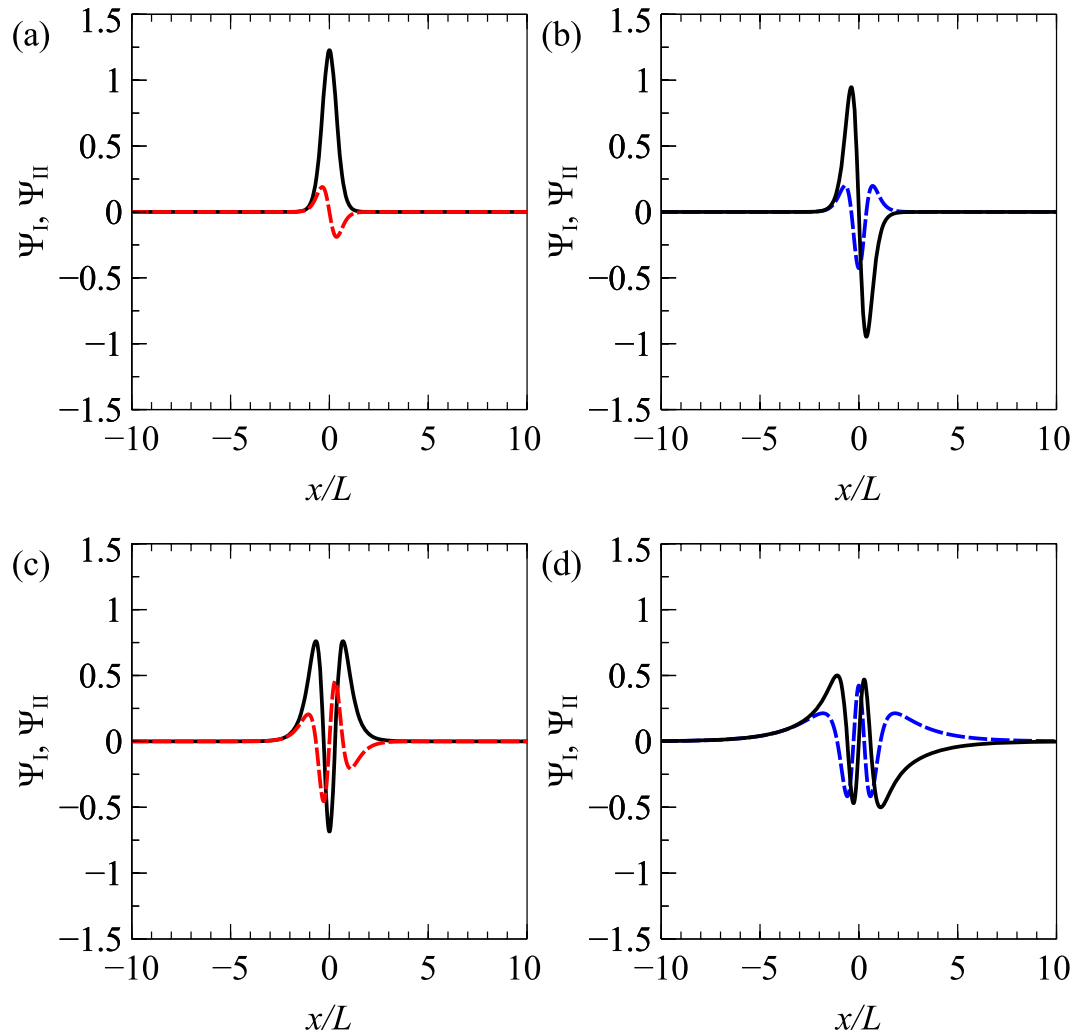
Figure 3. The normalized zero-energy bound-state wavefunctions of the symmetric Pöschl-Teller potential, for strength $a = 24$. (**a**), (**b**), (**c**) and (**d**) correspond to the case of $\Delta = 0.597$, 2.276, 3.817 and 5.282, respectively. The dashed-red and dashed-blue lines correspond to Ψ_{I}, while the solid-black lines correspond to Ψ_{II}.

$$\lambda_{1N}(c) = cq + 1 - \frac{1}{8}(q^2 + 5) - \frac{q}{64c}(q^2 + 11 - 32) + O(c^{-2}), \tag{23}$$

where $N = 1, 2, 3, \ldots$ and $q = 2N - 1$[93]. Keeping only the terms of expansion shown in Eq. (23) yields the following eigenvalues:

$$E = -\frac{1}{2}(1 - 2N) - \frac{a}{8} + \frac{1}{4a}[3 - (1 - 2N)^2], \tag{24}$$

where N is restricted to ensure that E is negative. The resulting approximate eigenvalues for the symmetric Pöschl-Teller potential of strength $a = 24$ are $E = -2.475$, -1.555 and -0.734 respectively, and are indicated as black crosses in Fig. 2. The approximate eigenvalues deviate increasingly from the numerically exact results, $E = -2.473$, -1.542 and -0.682, with decreasing y. It should be noted that a refinement of the approximate values of λ_{1N} can be found in ref. 93.

For the hyperbolic secant potential, $V = -V_0/\cosh(\tilde{x})$, it was found that there was a minimum potential strength of $V_0 = 1/2$, required to observe a zero-energy mode[22]. According to the Landauer formula, the conductance along the waveguide when the Fermi level is set to the Dirac point is $4ne^2/h$, where n is the number of zero-energy modes. The existence of a threshold in the potential strength needed for the waveguide to contain a zero-energy mode allowed us to suggest that such waveguides could be used as switchable devices. However, later numerical calculations utilizing a variable phase method implied that power-decaying potentials always possess a bound mode[58]. This result cast serious doubt in the validity of employing exponentially decaying potentials as a suitable model for graphene waveguides, since realistic potential profiles decay a power of distance rather than exponentially. Notably, the threshold potential strength at which the first zero-energy mode appears can be
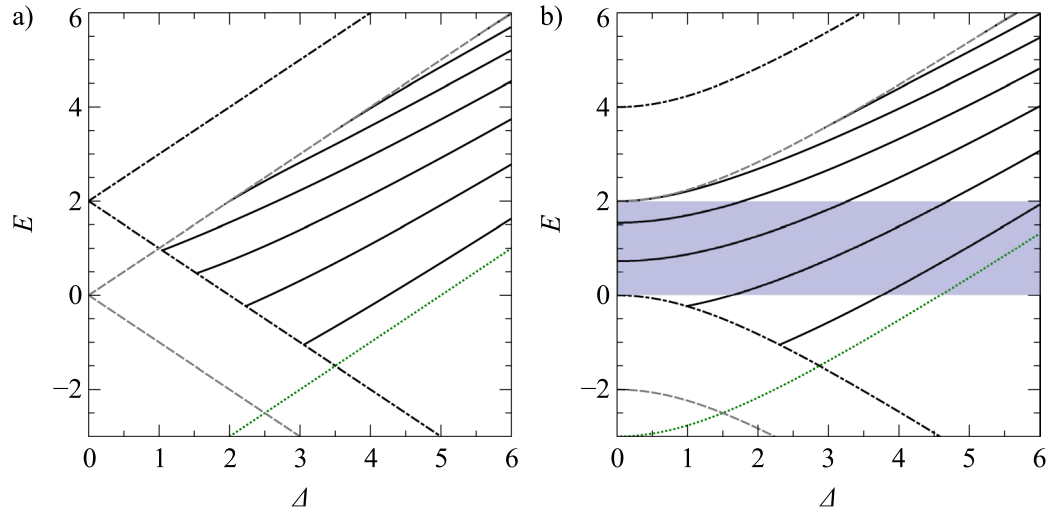
Figure 4. The energy spectra of confined states in the modified Pöschl-Teller potential, of strength $a = 24$ and $b = 2$, as a function of Δ for (**a**) $M = 0$ and (**b**) $M = 2$. The grey (dashed), black (dot-dashed) and green (dotted) lines correspond to $\Delta^2 + M^2 = E^2$, $\Delta^2 + M^2 = (E - b)^2$ and $\Delta^2 + M^2 = [E + (a - b)^2/4a]^2$, respectively. The blue-shaded area highlights the energy range in which the modes contained within the waveguide are non-leaky.

obtained from the condition of the first bound state coinciding with the first supercritical state, i.e. $E = -\Delta = 0$. In this instance, Eq. (21) can be solved exactly:

$$\Psi_{\mathrm{I}} = C_1 \cos\!\left(\int_0^{\tilde{x}} V(X)dX\right) + C_2 \sin\!\left(\int_0^{\tilde{x}} V(X)dX\right), \tag{25}$$

$$\Psi_{\mathrm{II}} = -C_1 \sin\!\left(\int_0^{\tilde{x}} V(X)dX\right) + C_2 \cos\!\left(\int_0^{\tilde{x}} V(X)dX\right). \tag{26}$$

For even modes of Ψ_{I}, $C_2 = 0$, whereas, for odd modes of Ψ_{I}, $C_1 = 0$. In the absence of the potential, when $E = \Delta = 0$ the two first order differential equations in Ψ_{I} and Ψ_{II} decouple, and Eq. (21) reduces to a first order differential equation. As $E = -\Delta \to 0$ and $x \to \pm\infty$ (where the potential is zero), Eq. (25) and Eq. (26) are required to be linearly dependent[94] and the Wronskian of the solutions Ψ_{I} and Ψ_{II} is zero[95]. Consequently, the bound modes satisfy the condition: $|\Psi_{\mathrm{I}}(\pm\infty)|^2 = |\Psi_{\mathrm{II}}(\pm\infty)|^2$. Therefore, the threshold potential strength at which the first zero-energy mode appears is found by the condition

$$\left| \int_0^{\infty} V(\tilde{x})d\tilde{x} \right| = \frac{\pi}{4}. \tag{27}$$

Therefore, for any square-integrable potential, the threshold for the appearance of the first bound state of zero energy is only a function of the integrated potential. Notably, this is the same result obtained as relativistic Levinson theorem[45, 59–62]. For the Pöschl-Teller potential, Eq. (27) yields $a = \pi$, which agrees with Eq. (18). For $V = -V_0/\cosh(\tilde{x})$, Eq. (27) yields $V_0 = 1/2$ which restores the result of ref. 22. This result implies that square-integrable power decaying potentials do indeed have a threshold, in contrast to the numerically predicted result of ref. 58. In this respect, exponentially decaying potentials are not that different from power-decaying and are perfectly suitable for the modeling of top-gated Weyl semimetals.

Finally, it should be noted that in the non-relativistic limit, Eq. (10) restores the well known results[14] for the bound state functions of the Schrödinger equation for the Pöschl-Teller potential. In the limit that α and δ are much smaller than β and γ (i.e. large Δ):

$$\lim_{\Delta \to \infty} (H(\alpha, \beta, \gamma, \delta, \eta, Z)) = Z^{-\beta} \,_2F_1(Q, \ 1 + \gamma - \beta - Q; \ 1 + \gamma; \ 1 - Z), \tag{28}$$

where $Q = \left(1 + \gamma - \beta \pm \sqrt{1 + \gamma^2 + \beta^2 - 4(\eta_s + \delta_s)}\right)/2$ and $_2F_1$ is the Gauss hypergeometric function. Substituting $E = E_{\mathrm{SE}} + \Delta$, $b = 0$ and $s_\beta = -s_\gamma = 1$ into Eq. (10), results in the non-relativistic bound state functions

$$\lim_{\Delta \to \infty} (\Psi_{\mathrm{I}}) \propto \,_2F_1(\varepsilon + 1 + T, \varepsilon - T; 1 + \varepsilon; \ 1 - Z)Z^{\frac{\varepsilon}{2}}(1 - Z)^{\frac{\varepsilon}{2}}, \tag{29}$$

where $\varepsilon = s_\beta\sqrt{-2E_{\mathrm{SE}}\Delta}$ and $T = (-1 + \sqrt{1 + 2a\Delta})/2$. For the solutions to be finite at $Z = 0$, we require that $\varepsilon - T = -N$ where $N = 0, 1, 2, \ldots$. When this criteria is met, the Gauss hypergeometric function is a polynomial of degree N and the energy levels are given by
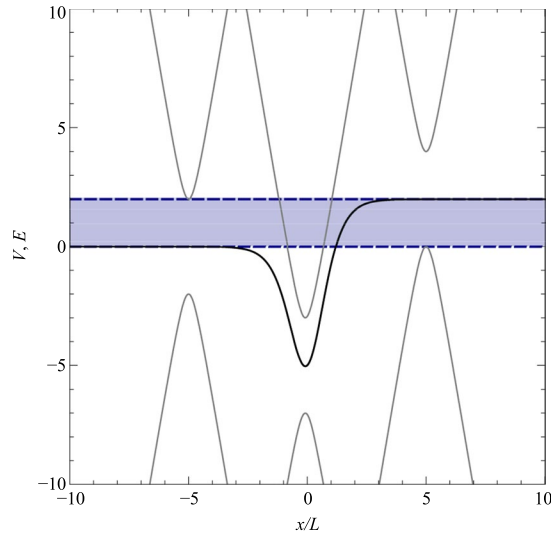
Figure 5. Schematic diagrams of the dispersion of a gaped Dirac material. The black lines represent the modified Pöschl-Teller potential profile, of strength $a = 24$ and $b = 2$. The grey lines represent the charge-carrier dispersion of particles of $M = 2$. The blue shaded area represent the energy range in which there are no continuum states to couple to outside of the well.

$$E_{SE} = -\frac{1}{8\Delta}[-(1 + 2N) + \sqrt{1 + 2a\Delta}]^2. \tag{30}$$

Modified Pöschl-Teller potential solutions.   We shall now consider the case of finite b, which represents a smooth asymmetric waveguide. Previously considered asymmetric waveguides varied abruptly on the same scale as the graphene lattice constant[54, 96–99]. We shall now consider more realistic smooth asymmetric waveguides, which fit closer to experimentally achievable potential profiles. In Fig. 4, we plot the energy spectrum for the potential defined by the parameters $a = 24$ and $b = 2$. The introduction of the asymmetry term b reduces the number of modes at $E = 0$, which are now quasi-bound modes for the massless case (Fig. 4a), since they can couple to continuum states outside of the waveguide. Naturally, for massive Dirac fermions full confinement is possible across a range of energies. In Fig. 5, we show a schematic diagram of the dispersion of a gapped Dirac material, subjected to the modified Pöschl-Teller potential defined by $a = 24$ and $b = 2$. For a particle of mass $M = 2$, it can be seen that for the energy range $E = 0$ to $E = 2$ there are no continuum states outside of the well, therefore in that range all bound solutions will be non-leaky. The corresponding energy spectrum of confined states is shown in Fig. 4b.

Conclusions
We have analyzed the behavior of quasi-relativistic two-dimensional particles subjected to a modified Pöschl-Teller potential. Our results have direct applications to electronic waveguides in 2D Dirac materials. For the symmetric Pöschl-Teller potential, explicit forms were obtained for the eigenvalues of supercritical states. A universal expression, for any symmetric potential, was obtained for the critical potential strength required to observe the first zero-energy state. The well known results for the Pöschl-Teller potential are recovered in the non-relativistic limit.

References
 1. Pöschl, G. & Teller, E. Bemerkungen zur quantenmechanik des anharmonischen oszillators. *Zeitschrift für Physik A Hadrons and Nuclei* **83**, 143–151 (1933).
 2. Dong, S.-H. *Factorization method in quantum mechanics*, vol. 150 (Springer Science & Business Media, 2007).
 3. Sutherland, B. & Römer, R. A. Exciton, spinon, and spin wave modes in a soluble one-dimensional many-body system. *Phys. Rev. Lett.* **71**, 2789–2792 (1993).
 4. Römer, R. A. & Sutherland, B. Critical exponents for the sinh-cosh interaction model in the zero sector. *Phys. Rev. B* **49**, 6779–6787 (1994).
 5. Römer, R. A. & Sutherland, B. Transport properties of a one-dimensional two-component quantum liquid with hyperbolic interactions. *Phys. Rev. B* **50**, 15389–15392 (1994).
 6. Ferrari, V. & Mashhoon, B. New approach to the quasinormal modes of a black hole. *Phys. Rev. D* **30**, 295 (1984).
 7. Berti, E., Cardoso, V. & Starinets, A. O. Quasinormal modes of black holes and black branes. *Classical and Quantum Gravity* **26**, 163001 (2009).
 8. Kogelnik, H. 2. Theory of dielectric waveguides. In *Integrated optics*, 13–81 (Springer, 1975).
 9. Radovanović, J., Milanović, V., Ikonić, Z. & Indjin, D. Intersubband absorption in Pöschl–Teller-like semiconductor quantum wells. *Phys. Lett. A* **269**, 179–185 (2000).
10. Yldrm, H. & Tomak, M. Nonlinear optical properties of a Pöschl-Teller quantum well. *Phys. Rev. B* **72**, 115340 (2005).
11. Baizakov, B. B. & Salerno, M. Delocalizing transition of multidimensional solitons in Bose-Einstein condensates. *Phys. Rev. A* **69**, 013602 (2004).
12. Antezza, M., Dalfovo, F., Pitaevskii, L. P. & Stringari, S. Dark solitons in a superfluid Fermi gas. *Phys. Rev. A* **76**, 043610 (2007).

13. Dutt, R., Khare, A. & Sukhatme, U. P. Supersymmetry, shape invariance, and exactly solvable potentials. *Am. J. Phys.* **56**, 163–168 (1988).
14. Landau, L. D. & Lifshitz, E. M. *Quantum mechanics: non-relativistic theory*, vol. 3 of Course of Theoretical Physics (Pergamon Press, Oxford, 1977).
15. Jia, C. S., Guo, P., Diao, Y. F., Yi, L. Z. & Xie, X. J. Solutions of Dirac equations with the Pöschl-Teller potential. *Eur. Phys. J. A* **34**, 41–48 (2007).
16. Xu, Y., He, S. & Jia, C.-S. Approximate analytical solutions of the Dirac equation with the Pöschl–Teller potential including the spin–orbit coupling term. *J. Phys. A* **41**, 255302 (2008).
17. Wei, G.-F. & Dong, S.-H. The spin symmetry for deformed generalized Pöschl–Teller potential. *Phys. Lett. A* **373**, 2428–2431 (2009).
18. Wei, G.-F. & Dong, S.-H. Algebraic approach to pseudospin symmetry for the Dirac equation with scalar and vector modified Pöschl-Teller potentials. *Europhys. Lett.* **87**, 40004 (2009).
19. Jia, C.-S., Chen, T. & Cui, L.-G. Approximate analytical solutions of the Dirac equation with the generalized Pöschl–Teller potential including the pseudo-centrifugal term. *Phys. Lett. A* **373**, 1621–1626 (2009).
20. Miranda, M., Sun, G.-H. & Dong, S.-H. The solution of the second Pöschl–Teller like potential by Nikiforov–Uvarov method. *Int. J. Mod. Phys. B* **19**, 123–129 (2010).
21. Taşkn, F. & Koçak, G. Spin symmetric solutions of Dirac equation with Pöschl-Teller potential. *Chin. Phys. B* **20**, 070302 (2011).
22. Hartmann, R. R., Robinson, N. J. & Portnoi, M. E. Smooth electron waveguides in graphene. *Phys. Rev. B* **81**, 245431 (2010).
23. Hartmann, R. R. & Portnoi, M. E. Quasi-exact solution to the Dirac equation for the hyperbolic-secant potential. *Phys. Rev. A* **89**, 012101 (2014).
24. Hartmann, R. R., Shelykh, I. A. & Portnoi, M. E. Excitons in narrow-gap carbon nanotubes. *Phys. Rev. B* **84**, 035437 (2011).
25. Park, C.-S. Two-dimensional transmission through modified Pöschl-Teller potential in bilayer graphene. *Phys. Rev. B* **92**, 165422 (2015).
26. Wehling, T., Black-Schaffer, A. M. & Balatsky, A. V. Dirac materials. *Adv. Phys* **63**, 1–76 (2014).
27. Neto, A. H. C., Guinea, F., Peres, N. M. R., Novoselov, K. S. & Geim, A. K. The electronic properties of graphene. *Rev. Mod. Phys.* **81**, 109 (2009).
28. Charlier, J.-C., Blase, X. & Roche, S. Electronic and transport properties of nanotubes. *Rev. Mod. Phys.* **79**, 677 (2007).
29. Hasan, M. Z. & Kane, C. L. Colloquium: topological insulators. *Rev. Mod. Phys.* **82**, 3045 (2010).
30. Qi, X.-L. & Zhang, S.-C. Topological insulators and superconductors. *Zhang, Rev. Mod. Phys.* **83**, 1057 (2011).
31. Zazunov, A., Egger, R. & Levy Yeyati, A. Low-energy theory of transport in Majorana wire junctions. *Phys. Rev. B* **94**, 014502 (2016).
32. Xiao, D., Liu, G.-B., Feng, W., Xu, X. & Yao, W. Coupled spin and valley physics in monolayers of MoS_2 and other group-VI dichalcogenides. *Phys. Rev. Lett.* **108**, 196802 (2012).
33. Young, S. M. *et al*. Dirac semimetal in three dimensions. *Phys. Rev. Lett.* **108**, 140405 (2012).
34. Coulter, B. L. & Adler, C. G. The relativistic one-dimensional square potential. *Am. J. Phys.* **39**, 305–309 (1971).
35. Calogeracos, A., Dombey, N. & Imagawa, K. Yadernaya fiz. 159, 1331 (1996). *Phys. At. Nuc.* **159**, 1275 (1996).
36. Dong, S.-H., Hou, X.-W. & Ma, Z.-Q. Relativistic Levinson theorem in two dimensions. *Phys. Rev. A* **58**, 2160–2167 (1998).
37. Dombey, N., Kennedy, P. & Calogeracos, A. Supercriticality and transmission resonances in the Dirac equation. *Phys. Rev. Lett* **85**, 1787 (2000).
38. Kennedy, P. The Woods–Saxon potential in the Dirac equation. *J. Phys. A: Math. Gen.* **35**, 689 (2002).
39. Villalba, V. M. & Greiner, W. Transmission resonances and supercritical states in a one-dimensional cusp potential. *Phys. Rev. A* **67**, 052707 (2003).
40. Kennedy, P., Dombey, N. & Hall, R. L. Phase shifts and resonances in the Dirac equation. *Int. J. Mod. Phys. A.* **19**, 3557–3581 (2004).
41. Guo, J., Yu, Y. & Jin, S. Transmission resonance for a Dirac particle in a one-dimensional Hulthén potential. *Cent. Eur. J. Phys.* **7**, 168–174 (2009).
42. Villalba, V. M. & González-Árraga, L. A. Tunneling and transmission resonances of a Dirac particle by a double barrier. *Phys. Scr.* **81**, 025010 (2010).
43. Sogut, K. & Havare, A. Transmission resonances in the Duffin–Kemmer–Petiau equation in $(1 + 1)$ dimensions for an asymmetric cusp potential. *Phys. Scr.* **82**, 045013 (2010).
44. Arda, A., Aydoğdu, O. & Sever, R. Scattering and bound state solutions of the asymmetric Hulthén potential. *Phys. Scr.* **84**, 025004 (2011).
45. Miserev, D. Analytical study of bound states in graphene nanoribbons and carbon nanotubes: The variable phase method and the relativistic Levinson theorem. *J. Exp. Theor. Phys* **122**, 1070–1083 (2016).
46. Katsnelson, M. I., Novoselov, K. S. & Geim, A. K. Chiral tunnelling and the Klein paradox in graphene. *Nat. Phys.* **2**, 620–625 (2006).
47. Tudorovskiy, T. Y. & Chaplik, A. Spatially inhomogeneous states of charge carriers in graphene. *JETP Lett.* **84**, 619–623 (2007).
48. Pereira, J. M., Mlinar, V., Peeters, F. M. & Vasilopoulos, P. Confined states and direction-dependent transmission in graphene quantum wells. *Phys. Rev. B* **74**, 045424 (2006).
49. Nguyen, H. C., Hoang, M. T. & Nguyen, V. L. Quasi-bound states induced by one-dimensional potentials in graphene. *Phys. Rev. B* **79**, 035411 (2009).
50. Zhang, F.-M., He, Y. & Chen, X. Guided modes in graphene waveguides. *Appl. Phys. Lett.* **94**, 212105 (2009).
51. Williams, J., Low, T., Lundstrom, M. & Marcus, C. Gate-controlled guiding of electrons in graphene. *Nat. Nanotechnol.* **6**, 222–225 (2011).
52. Yuan, J.-H., Cheng, Z., Zeng, Q.-J., Zhang, J.-P. & Zhang, J.-J. Velocity-controlled guiding of electron in graphene: Analogy of optical waveguides. *J. Appl. Phys.* **110**, 103706 (2011).
53. Wu, Z. Electronic fiber in graphene. *Appl. Phys. Lett.* **98**, 082117 (2011).
54. Ping, P., Peng, Z., Jian-Ke, L., Zhen-Zhou, C. & Guan-Qiang, L. Oscillating guided modes in graphene-based asymmetric waveguides. *Commun. Theor. Phys.* **58**, 765 (2012).
55. Tudorovskiy, T., Reijnders, K. & Katsnelson, M. Chiral tunneling in single-layer and bilayer graphene. *Phys. Scr.* **2012**, 014010 (2012).
56. Cohnitz, L., De Martino, A., Häusler, W. & Egger, R. Chiral interface states in graphene *p*–*n* junctions. *Phys. Rev. B* **94**, 165443 (2016).
57. Jiang, B.-Y. *et al*. Tunable plasmonic reflection by bound 1D electron states in a 2D Dirac metal. *Phys. Rev. Lett.* **117**, 086801 (2016).
58. Stone, D., Downing, C. & Portnoi, M. Searching for confined modes in graphene channels: The variable phase method. *Phys. Rev. B* **86**, 075464 (2012).
59. Clemence, D. P. Low-energy scattering and Levinson's theorem for a one-dimensional Dirac equation. *Inverse Probl.* **5**, 269 (1989).
60. Lin, Q.-g Levinson theorem for Dirac particles in one dimension. *Eur. Phys. J. D* **7**, 515–524 (1999).
61. Calogeracos, A. & Dombey, N. Strong Levinson theorem for the Dirac equation. *Phys. Rev. Lett.* **93**, 180405 (2004).
62. Ma, Z.-Q., Dong, S.-H. & Wang, L.-Y. Levinson theorem for the Dirac equation in one dimension. *Phys. Rev. A* **74**, 012712 (2006).
63. Dirac, P. A. The quantum theory of the electron. In *Proc. R. Soc. Lond. Ser. A*, vol. 117, 610–624 (The Royal Society, 1928).
64. Wallace, P. R. The band theory of graphite. *Phys. Rev.* **71**, 622 (1947).
65. Dutta, S. & Pati, S. K. Novel properties of graphene nanoribbons: a review. *J. Mater. Chem* **20**, 8207–8223 (2010).
66. Chung, H.-C., Chang, C.-P., Lin, C.-Y. & Lin, M.-F. Electronic and optical properties of graphene nanoribbons in external fields. *Phys. Chem. Chem. Phys.* **18**, 7573–7616 (2016).
67. Portnoi, M. E., Kibis, O. V. & Rosenau da Costa, M. Terahertz applications of carbon nanotubes. *Superlattice Microst.* **43**, 399–407 (2008).
68. Hartmann, R. R. & Portnoi, M. E. *Optoelectronic Properties of Carbon-based Nanostructures: Steering electrons in graphene by electromagnetic fields* (LAP LAMBERT Academic Publishing, Saarbrucken, 2011).

69. Hartmann, R. R., Kono, J. & Portnoi, M. E. Terahertz science and technology of carbon nanomaterials. *Nanotechnology* **25**, 322001 (2014).
70. Hartmann, R. R. & Portnoi, M. E. Terahertz transitions in quasi-metallic carbon nanotubes. *IOP Conf. Ser.: Mater. Sci. Eng.* **79**, 12014–12018 (2015).
71. Liu, C.-C., Jiang, H. & Yao, Y. Low-energy effective Hamiltonian involving spin-orbit coupling in silicene and two-dimensional germanium and tin. *Phys. Rev. B* **84**, 195430 (2011).
72. Hills, R. D. Y., Kusmartseva, A. & Kusmartsev, F. V. Current-voltage characteristics of Weyl semimetal semiconducting devices, Veselago lenses, and hyperbolic Dirac phase. *Phys. Rev. B* **95**, 214103 (2017).
73. Giovannetti, G., Khomyakov, P. A., Brocks, G., Kelly, P. J. & Van Den Brink, J. Substrate-induced band gap in graphene on hexagonal boron nitride: Ab initio density functional calculations. *Phys. Rev. B* **76**, 073103 (2007).
74. Nieto, M. M. Exact wave-function normalization constants for the $B_0 \tanh z - U_0 \cosh^{-2} z$ and Pöschl-Teller potentials. *Phys. Rev. A* **17**, 1273–1283 (1978).
75. Turbiner, A. V. Quantum mechanics: problems intermediate between exactly solvable and completely unsolvable. *Soviet Phys. JETP* **67**, 230–236 (1988).
76. Ushveridze, A. G. *Quasi-exactly solvable models in quantum mechanics* (CRC Press, 1994).
77. Bender, C. M. & Boettcher, S. Quasi-exactly solvable quartic potential. *J. Phys. A* **31**, L273 (1998).
78. Downing, C. A. On a solution of the Schrödinger equation with a hyperbolic double-well potential. *J. Math. Phys.* **54**, 072101 (2013).
79. Hartmann, R. R. Bound states in a hyperbolic asymmetric double-well. *J. Math. Phys.* **55**, 012105 (2014).
80. Hartmann, R. R. & Portnoi, M. E. Exciton states in narrow-gap carbon nanotubes. *AIP Conf. Proc.* **1705** (2016).
81. Hartmann, R. R. & Portnoi, M. E. Pair states in one-dimensional Dirac systems. *Phys. Rev. A* **95**, 062110 (2017).
82. Miserev, D. S. & Entin, M. V. Quantum mechanics of graphene with a one-dimensional potential. *J. Exp. Theor. Phys.* **115**, 694–705 (2012).
83. Reijnders, K., Tudorovskiy, T. & Katsnelson, M. Semiclassical theory of potential scattering for massless Dirac fermions. *Ann. Phys.* **333**, 155–197 (2013).
84. Heun, K. Zur theorie der riemann'schen functionen zweiter ordnung mit vier verzweigungspunkten. *Math. Ann* **33**, 161–179 (1889).
85. Xie, Q., Zhong, H., Batchelor, M. T. & Lee, C. The quantum Rabi model: solution and dynamics. *J. Phys. A: Math. Theor.* **50**, 113001 (2017).
86. Ramazan Koç, M. K. & Tütüncüler, H. Quasi exact solution of the Rabi Hamiltonian. *J. Phys. A: Math. Theor.* **35**, 9425 (2002).
87. Reik, H. G. & Doucha, M. Exact solution of the Rabi Hamiltonian by known functions? *Phys. Rev. Lett.* **57**, 787–790 (1986).
88. Zhong, H., Xie, Q., Batchelor, M. T. & Lee, C. Analytical eigenstates for the quantum Rabi model. *J. Phys. A: Math. Theor.* **46**, 415302 (2013).
89. Maciejewski, A. J., Przybylska, M. & Stachowiak, T. Full spectrum of the Rabi model. *Phys. Lett. A* **378**, 16–20 (2014).
90. Ronveaux, A. & Arscott, F. M. *Heun's differential equations* (Oxford University Press, 1995).
91. Fiziev, P. P. Novel relations and new properties of confluent Heun's functions and their derivatives of arbitrary order. *J. Phys. A* **43**, 035203 (2009).
92. Shahnazaryan, V. A., Ishkhanyan, T. A., Shahverdyan, T. A. & Ishkhanyan, A. M. New relations for the derivative of the confluent Heun function. *Armenian Journal of Physics* **5**, 146 (2012).
93. Abramowitz, M. *Handbook of Mathematical Functions, With Formulas, Graphs, and Mathematical Tables* (Dover Publications, Incorporated, 1974).
94. Kennedy, P. & Dombey, N. Low momentum scattering in the Dirac equation. *J. Phys. A: Math. Theor.* **35**, 6645 (2002).
95. Calogero, F. *Variable Phase Approach to Potential Scattering by F Calogero*, vol. 35 (Elsevier, 1967).
96. He, Y., Xu, Y., Yang, Y. & Huang, W. Guided modes in asymmetric graphene waveguides. *Appl. Phys. A* **115**, 895–902 (2014).
97. Xu, Y. & Ang, L. Guided modes in a triple-well graphene waveguide: analogy of five-layer optical waveguide. *J. Opt* **17**, 035005 (2015).
98. Salem, E. B., Chaabani, R. & Jaziri, S. Mid/far-infrared photo-detectors based on graphene asymmetric quantum wells. *Chin. Phys. B* **25**, 098101 (2016).
99. Xu, Y. & Ang, L. K. Guided modes in a double-well asymmetric potential of a graphene waveguide. *Electronics* **5**, 87 (2016).

Acknowledgements

Author Contributions

R.R.H. and M.E.P. wrote the main manuscript text and R.R.H. prepared the figures. All authors reviewed the manuscript.

Additional Information

Competing Interests: The authors declare that they have no competing interests.

Publisher's note: Springer Nature remains neutral with regard to jurisdictional claims in published maps and institutional affiliations.